CHANNELS
2016, VOL. 10, NO. 5, 346–354
http://dx.doi.org/10.1080/19336950.2016.1186318

Taylor & Francis
Taylor & Francis Group

SHORT COMMUNICATION

A $Ca_v3.2$/Stac1 molecular complex controls T-type channel expression at the plasma membrane

Yuriy Rzhepetskyy[a], Joanna Lazniewska[a], Juliane Proft[a], Marta Campiglio[b], Bernhard E. Flucher[b], and Norbert Weiss[a]

[a]Institute of Organic Chemistry and Biochemistry, Academy of Sciences of the Czech Republic, Prague, Czech Republic; [b]Division of Physiology, Department of Physiology and Medical Physics, Medical University Innsbruck, Innsbruck, Austria

ABSTRACT

Low-voltage-activated T-type calcium channels are essential contributors to neuronal physiology where they play complex yet fundamentally important roles in shaping intrinsic excitability of nerve cells and neurotransmission. Aberrant neuronal excitability caused by alteration of T-type channel expression has been linked to a number of neuronal disorders including epilepsy, sleep disturbance, autism, and painful chronic neuropathy. Hence, there is increased interest in identifying the cellular mechanisms and actors that underlie the trafficking of T-type channels in normal and pathological conditions. In the present study, we assessed the ability of Stac adaptor proteins to associate with and modulate surface expression of T-type channels. We report the existence of a $Ca_v3.2$/Stac1 molecular complex that relies on the binding of Stac1 to the amino-terminal region of the channel. This interaction potently modulates expression of the channel protein at the cell surface resulting in an increased T-type conductance. Altogether, our data establish Stac1 as an important modulator of T-type channel expression and provide new insights into the molecular mechanisms underlying the trafficking of T-type channels to the plasma membrane.

ARTICLE HISTORY
Received 29 April 2016
Accepted 29 April 2016

KEYWORDS
$Ca_v3.2$ channel; Stac adaptor protein; trafficking; T-type calcium channel

Introduction

T-type channels are low-voltage-activated calcium channels widely expressed throughout the nervous system (for review see [1]). Their low activation threshold makes these channels perfectly suited to operate around the resting electrical membrane potential of neurons where they play an essential role in regulating cellular excitability. They provide a "window current" that supports passive Ca^{2+} entry,[2] which contributes to the resting membrane potential,[3] and influencing the excitability threshold of nerve cells. Although a significant fraction of T-type channels are inactivated at rest, their recovery from inactivation during brief periods of hyperpolarization generates rebound burst of action potentials that contribute to various forms of neuronal rhythmogenesis.[4-8] In addition, their ability to associate with and modulate a number of potassium channel conductances further positions T-type channels to shape and fine tune the firing of nerve cells.[9-12] Besides their implication in the control of intrinsic neuronal excitability, T-type channels also associate with the vesicular release machinery to support a low-threshold form of exocytosis.[13,14] Aberrant expression of T-type channels has been reported in a number of pathological situations including painful neuropathy arising from diabetes,[15-18] inflammatory,[19] and nerve injury conditions.[20] In addition, up-regulation of T-type channels is responsible for epileptic seizures in several rodent models of epilepsy.[21-26] Although a number of signaling pathways regulating T-type channel activity have been reported,[27] the molecular mechanisms and signaling molecules controlling the trafficking, sorting, and expression of the channel protein at the plasma membrane remain largely unknown.

Stac proteins form a family of SH3 and cysteine-rich domain-containing proteins whose primary functions remain largely unknown.[28] Three genes encode for mammalian Stac proteins (Stac1, −2, and −3) with specific tissue expression profiles. Stac3 is essentially expressed in skeletal muscle where it plays an important role in the trafficking of $Ca_v1.1$ channels,[29,30] and

CONTACT Norbert Weiss weiss@uochb.cas.cz Institute of Organic Chemistry and Biochemistry, Ion Channels and Diseases Group, Flemingovo nám. 2., Prague 16610, Czech Republic.

Color versions of one or more of the figures in the article can be found online at www.tandfonline.com/kchl.

is therefore essential for the assembly of the excitation-contraction coupling machinery [31,32] and the maturation of skeletal muscle cells.[33] In contrast, Stac1 and Stac2 are primarily found in nerve cells, including a number of subset of DRG neurons.[34] For instance, transcripts for Stac1 were found predominantly in nociceptive peptidergic neurons, whereas Stac2 was identified in a subset of nonpeptidergic nociceptors, in $trkB^+$ neurons, and in a subpopulation of proprioceptive neurons.[34] Stac1 and Stac2 are also present in different brain regions including the cerebellum and fore-/midbrain.

Given the implication of T-type channels in neuronal excitability, and the abundance of Stac in nerve cells, we assessed the ability of Stac1 to associate with and modulate expression of $Ca_v3.2$ channels. We reveal the existence of a Stac1/$Ca_v3.2$ T-type calcium channel molecular complex that relies on the binding of Stac1 to the amino-terminal region of the channel. This interaction of Stac1 with $Ca_v3.2$ modulates T-type currents by enhancing expression of the channel protein at the cell surface.

Results

Stac1 associates with $Ca_v3.2$ channels

To determine whether T-type calcium channels and Stac associate at the protein level, we performed co-immunoprecipitations from tsA-201 cells expressing GFP-tagged human $Ca_v3.2$ channels (GFP-$hCa_v3.2$) together with mCherry-tagged Stac1 (mCherry-Stac1). Specific anti-GFP antibody precipitated GFP-$hCa_v3.2$ with mCherry-Stac1, revealing the existence of a Stac1/$Ca_v3.2$ molcular complex (Fig. 1A). To identify the $Ca_v3.2$ molcular determinants of Stac1 interactions, we assessed the ability of several intracellular regions of $hCa_v3.2$ to interact with Stac1. The main cytoplasmic domains of $hCa_v3.2$ fused to the GFP (Fig. 1B) were co-expressed in tsA-201 cells with Myc-tagged Stac1 (Myc-Stac1). Co-immunoprecipitation experiments revealed that Stac1 specifically immunoprecipitated with the amino-terminal region of $hCa_v3.2$ channels (Fig. 1C). To further map the binding of Stac1 within the amino-terminal region of $hCa_v3.2$, co-immunoprecipitation experiments were performed using GFP-tagged fusion proteins corresponding to the proximal (amino acids 1–50) and distal (amino acids 51–100) regions of the amino-terminal domain of $hCa_v3.2$ (Fig. 1B). As shown in Figure 1D, Stac1 specifically interacted with the distal region of the $hCa_v3.2$ N-terminal domain.

Collectively, these results demonstrate the existence of a $Ca_v3.2$/Stac1 complex that relies on the binding of Stac1 to the distal region of the amino-terminal domain of the channel.

Stac1 modulates surface expression of $hCa_v3.2$ channels

To analyze whether binding of Stac1 to $hCa_v3.2$ affects expression of the channel at the plasma membrane, we examined expression of $hCa_v3.2$ channels by immunostaining, using an exofacial hemagglutinin (HA)-tagged $hCa_v3.2$ (HA-$hCa_v3.2$). The expression of HA-$hCa_v3.2$ was quantified from low-magnification images obtained from non-permeabilized and permeabilized cells to assess surface and total expression of the channel, respectively (Fig. 2A). Immunostaining from non-permeabilized cells revealed a 67% increased ($p \leq 0.001$) surface expression of $hCa_v3.2$ in cells expressing Stac1 (Fig. 2B). In contrast, the total expression of the channel assessed from permeabilized cells expressing Stac1 remained unchanged compared to cells expressing the channel alone, suggesting that Stac1 enhanced surface expression of T-type channels independently of an effect on the overall expression levels of the channel protein. To confirm the functional expression of T-type channels at the cell surface, we performed patch-clamp recordings on tsA-201 cells expressing $hCa_v3.2$ channels. Representative Ba^{2+} current traces in response to 150 ms depolarizing steps to values ranging between −90 mV and +30 mV, from a holding potential of −100 mV, are shown in Figure 2C for $hCa_v3.2$ and $hCa_v3.2$/Stac1-expressing cells. Figure 2D shows the corresponding mean peak Ba^{2+} current density as a function of membrane voltage. Consistent with the increased surface expression of $hCa_v3.2$ in the presence of Stac1, T-type currents recorded from cells expressing Stac1 were significantly increased compared to cells expressing the channel alone. For instance, in response to a depolarizing pulse to 30 mV, the mean peak current density was increased by 52% ($p \leq 0.001$) in cells expressing Stac1 (35.5 ± 3.0 pA/pF, $n = 29$) compared to cells expressing $hCa_v3.2$ alone (23.4 ± 3.0 pA/pF, $n = 22$). The maximal macroscopic conductance was increased by 58% ($p \leq 0.001$) in cells expressing Stac1 (686 ± 56 pS/pF, $n = 29$) compared to cells expressing the channel alone (433 ± 51 pS/pF, $n = 22$) (Fig. 2D,

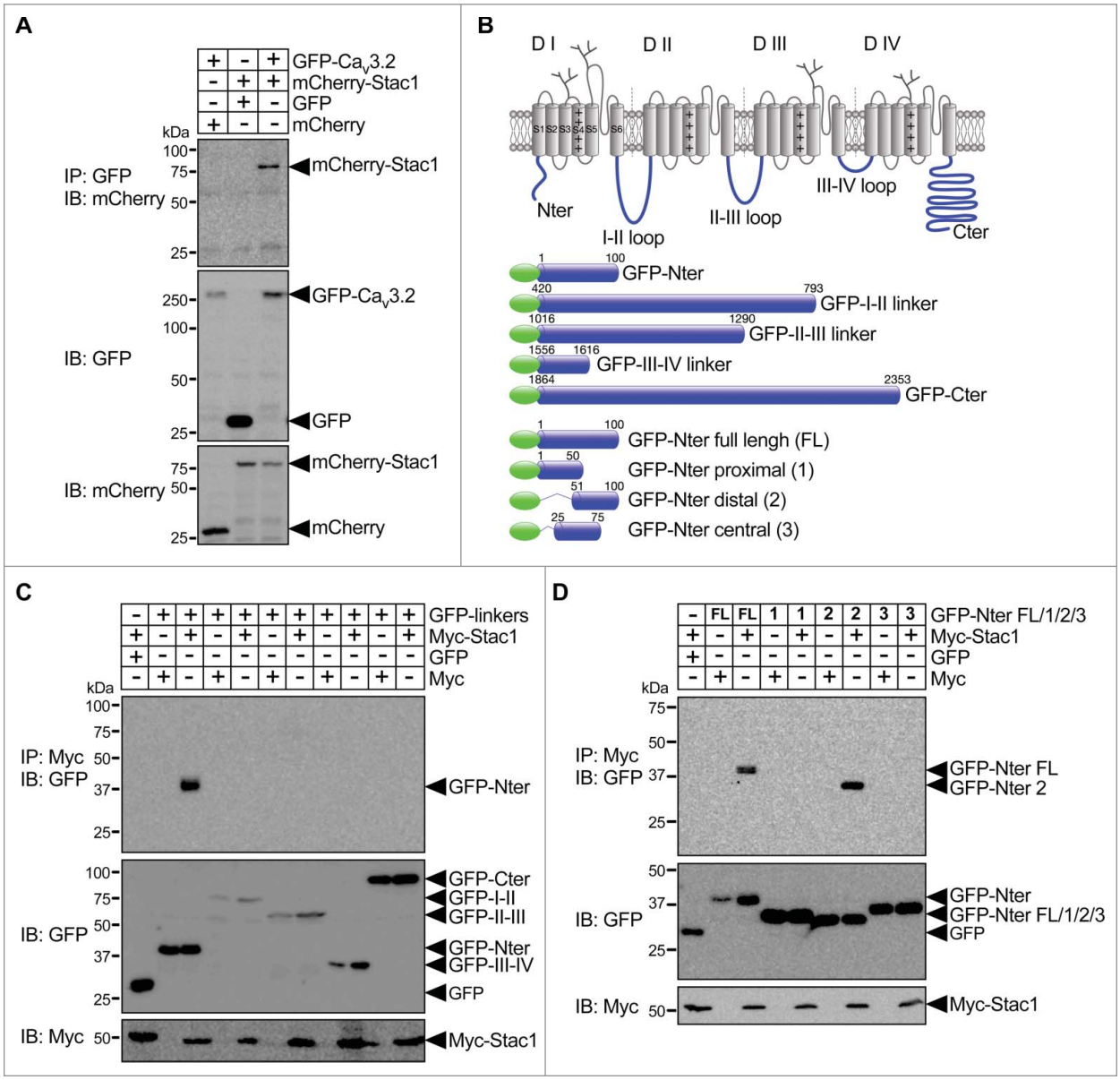

Figure 1. Stac1 associates with hCa$_v$3.2 channels. (A) Co-immunoprecipitation of mCherry-tagged Stac1 from tsA-201 cells co-transfected with GFP-tagged human Ca$_v$3.2 channel (GFP-hCa$_v$3.2). The upper panel shows the result of the co-immunoprecipitation of mCherry-Stac1 with GFP-hCa$_v$3.2 using an anti-GFP antibody. The lower panels show the immunoblot of GFP-hCa$_v$3.2 and mCherry-Stac1 using an anti-GFP and anti-mCherry antibody, respectively. (B) Schematic representation of the different GFP-tagged constructs used and corresponding to the main intracellular regions of hCa$_v$3.2. (C) Co-immunoprecipitation of the GFP-tagged hCa$_v$3.2 main intracellular linkers (GFP-linkers) with Myc-tagged Stac1 (Myc-Stac1). The upper panel shows the result of the co-immunoprecipitation of GFP-hCa$_v$3.2 linkers with Myc-Stac1 using an anti-Myc antibody. The lower panels show the immunoblots of GFP-hCa$_v$3.2 linkers and Myc-Stac1 using an anti-GFP and anti-mCherry antibody, respectively. (D) Co-immunoprecipitation of the GFP-tagged hCa$_v$3.2 N-terminal constructs with Myc-Stac1.

inset). Consistent with a pure effect of Stac1 on the steady-state expression of hCa$_v$3.2 at the cell surface, other biophysical properties of hCa$_v$3.2 channels, including voltage-dependence of activation and current kinetics were unaltered (data not shown).

Altogether, these data indicate that Stac1 is an important chaperone of hCa$_v$3.2 that enhances the steady-state expression of the channel at the plasma membrane.

Discussion

In contrast to high-voltage-activated calcium channels whose trafficking and cell surface expression are

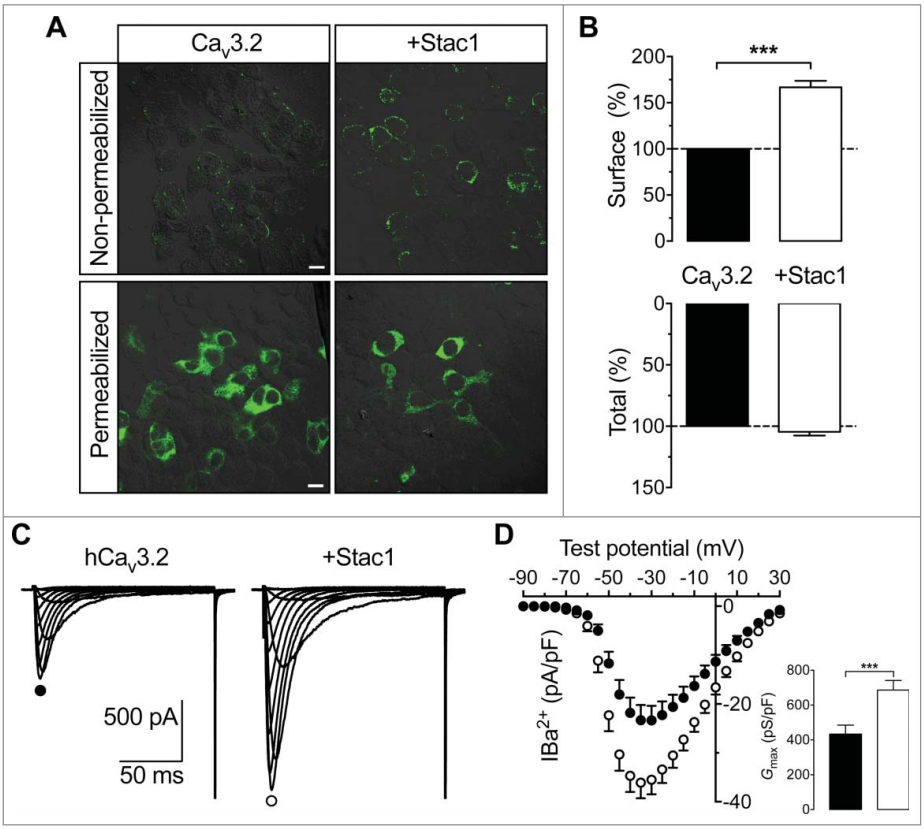

Figure 2. Stac1 enhances surface expression of hCa$_v$3.2 channels. (A) Low magnification confocal images of non-permeabilized (upper panels) and permeabilized (lower panels) tsA-201 cells expressing HA-tagged hCa$_v$3.2 channels alone (left panels) or together with Stac1 (right panels), and stained for HA-hCa$_v$3.2 (green) using a primary anti-HA antibody. (B) Corresponding mean surface (non-permeabilized) and total (permeabilized) expression of HA-hCa$_v$3.2 channels assessed by field fluorescence intensity measurement. (C) Representative Ba^{2+} current traces recorded from tsA-201 cells expressing HA-hCa$_v$3.2 channels alone (left panel) and in combination with Stac1 (right panel), in response to 150 ms depolarizing steps varied from −90 to +30 mV from a holding potential of −100 mV. (D) Corresponding mean current/voltage relationships for HA-hCa$_v$3.2 expressed alone (filled circles, $n = 22$) and in combination with Stac1 (open circles, $n = 29$). The inset represents the macroscopic conductance of tsA-201 cells expressing HA-hCa$_v$3.2 alone (black) and in combination with Stac1 (white).

controlled by their co-assembly with ancillary β- and $\alpha_2\delta$-subunits,[35,36] little is known about the molecular mechanisms and chaperone proteins involved in the expression of T-type channels. In the present study, we provide evidence for an important role of Stac in the control of T-type channel expression, and demonstrate that Stac1 forms a molecular complex with Ca$_v$3.2 that modulates surface expression of the channel.

Previous studies have reported a role of post-translational modifications, including asparagine-linked glycosylation and ubiquitination, in the control of T-type channel expression at the plasma membrane.[37-40] Moreover, the cytoplasmic I-II loop, in addition to its role in modulating gating properties of T-type channels,[41,42] was shown to influence the trafficking of the channel to the cell surface.[43,44] Here, we demonstrate that the chaperone protein Stac1 interacts with hCa$_v$3.2 channels. Detailed analysis of the molecular determinants of Ca$_v$3.2/Stac1 interaction revealed that Stac1 binds to the distal region of the cytoplasmic amino-terminal domain of hCa$_v$3.2. Of particular interest is the observation that binding of Stac1 to Ca$_v$3.2 significantly enhances surface expression of the channel protein, resulting in an increased macroscopic T-type calcium conductance. This observation is consistent with previous results obtained with the skeletal Ca$_v$1.1 channel, showing that Stac3 (the skeletal muscle-specific isoform) increases surface expression of the channel protein.[29,30]

There are different ways by which Stac1 may affect surface expression of hCa$_v$3.2 channels. Indeed, the steady-state expression of T-type channels at the cell surface results from a balance between channels

arriving at and being removed from the plasma membrane. One possible mechanism is that Stac1 could increase forward trafficking of the channel to the plasma membrane, possibly by masking an intracellular retention motif. However, no consensus endoplasmic reticulum retention motif is present in the amino-terminal region of $hCa_v3.2$. Alternatively, the increased surface expression of $hCa_v3.2$ channels in the presence of Stac1 could have resulted from an increased stability of the channel at the cell surface. Such a mechanism has been proposed for $Ca_v1.2$ and $Ca_v2.2$ channels where the ancillary β-subunit prevents ubiquitination and proteasomal degradation of the channel protein, and resulting in an increased expression of the channel.[45,46] Such a mechanism is perhaps unlikely for $Ca_v3.2$ channels for at least 2 reasons. First, $Ca_v3.2$ channels are ubiquitinated in the intracellular III-IV linker,[40,47] a region distant from the amino-terminal domain where Stac1 interacts with the channel. Second, if Stac1 had interfered with the proteasomal degradation of the channel, an increased total expression of the channel would have been expected. Nevertheless, regardless of the exact molecular mechanisms by which Stac1 enhances T-type channel expression, and given the importance of T-type channels in shaping neuronal electrical signals, the effect of Stac1 on the density of $Ca_v3.2$ channels at the cell surface is likely to have important consequences on neuronal excitability.

In summary, our data provide compelling evidence for an important role of Stac1 in the control of T-type channel expression at the plasma membrane, and enrich our understanding of the structural determinants and signaling molecules involved in the expression of T-type channels.

Material and methods

Plasmid cDNA constructs

The human wild-type HA-$Ca_v3.2$ construct (HA-$hCa_v3.2^{WT}$) [13] was used as a template to amplify by PCR the full length $Ca_v3.2$ and main cytoplasmic regions of the channel using the following primers: full-length $hCa_v3.2$: 5′AATACTCGAGCCATGACCGAGGGC3′ (forward) and 5′ACTCAAGCTTCTACACGGGGTCATCTGC3′ (reverse), Nterminal region: 5′ATTCTCGAGCCATGACCGAGGGCGCACGG3′ (forward) and 5′GAGAAGCTTTCATGGGTTGCAGACCAGCC3′ (reverse), Cterminal region: 5′ATTCTCGAGTAGAGGAGAGCAACAAGGAG3′ (forward) and 5′GAGAAGCTTTCACACGGGGTCATCTGCAC3′ (reverse), III linker: 5′ATTCTCGAGTAACGCAGTTCTCGGAGACG3′ (forward) and 5′GAGAAGCTTTCATGCTGTCCACGATGCGGC3′ (reverse), IIIII linker: 5′ATTCTCGAGTAACGCAGTTCTCGGAGACG3′ (forward) and 5′GAGAAGCTTTCATGCTGTCCACGATGCGGC3′ (reverse), IIIIV linker: 5′ATTCTCGAGTAAACTTCCACAAGTGCCG3′ (forward) and 5′GAGAAGCTTTCAGCTGGTGCACAGCGAGTG3′ (reverse), proximal Nterminal (amino acids 1-50): 5′ATTCTCGAGCCATGACCGAGGGCGCACGG3′ (forward) and 5′GAGAAGCTTTCAGGGTGACACGCCGAGCTC3′ (reverse), distal Nterminal (amino acids 51-100): 5′ATCTCGAGCCTCCGAGAGCCCGGCGGCCG3′ (forward) and 5′GAGAAGCTTTCATGGGTTGCAGACCAGCC3′ (reverse), central Nterminal (amino acids 25-75): 5′ATCTCGAGCCGTGGGGGCGTCCCCGGAGA3′ (forward) and 5′GAGAAGCTTTCACAAGGCCGGGTACGGGACG3′ (reverse). The PCR products were inserted into the XhoI/HindIII sites of the pEGFP-C1 vector. The coding sequence of Stac1 was isolated from mouse cortex cDNA. Primers were selected according to Genebank NM_016853. Briefly, a forward primer containing the KpnI restriction site upstream the start codon (5′GGTACCATGATTCCTCCAAGTGGCGCCCGC3′) and a reverse primer containing the BamHI restriction site before the stop codon (5′GGATCCATCACGTCTACCAGTACATCCAGT3′) were used to amplify by PCR the coding sequence of Stac1 (1209 bp), and the PCR product was inserted into KpnI/BamHI sites of the pc-GFP vector. The Stac1-GFP construct was then used as a PCR template to generated mCherry-tagged and Myc-tagged Stac1 constructs using the following primers: 5′GAGCTCGAGTAATGATTCCTCCAAGTGGCGC3′ (forward) and 5′CTTAAGCTTTCACACGTCTACCAGTACATC3′ (reverse). The PCR product was inserted into the XhoI/HindIII sites of the pEGFP-C1 vector. The GFP encoding sequence was then removed by NheI/XhoI sites and replaced by the mCherry encoding sequence amplified using the following primers: 5′TCCGCTAGCGCTACCGGTCGCCACCATGGTGAGCAAGGGCGAGGAGGATAACAT3′ (forward) and 5′TACTCGAGATCTGAGTCCGGACTTGTACAGCTCGTCCATGCCCCGGT3′ (reverse) or by the Myc encoding sequence amplified using

the following primers: 5′TCCGCTAGCGCTACCGGT CGCCACCATGGAACAAAAACTCATCTCAGAA GAGGATCTGGCTCGAGTAG3′ and 5′CTACTCGA GCCAGATCCTCTTCTGAGATGAGTTTTTGTTC CATGGTGGCGACCGGTAGCG CTAGCGGA3′. All final constructs were verified by sequencing of the full-length cDNA.

Cell culture and heterologous expression

Human embryonic kidney tsA-201 cells were grown in Dulbecco's modified Eagle's medium (DMEM) containing 10% fetal bovine serum and 1% penicillin/streptomycin (Invitrogen), and maintained under standard conditions at 37°C in a humidified atmosphere containing 5 % CO_2. Cells were transfected with plasmid cDNAs encoding $Ca_v3.2$ channel together with Stac1 using the calcium phosphate method.

Immunoprecipitation

Co-immunoprecipitations were performed 72 h after transfection. Cells were solubilized in 600 μL of lysis buffer (50 mM Tris/HCl, 0.05 mM EDTA, 10 mM Chaps; pH 7.5) supplemented with protease inhibitors cocktail (Roche). After sonication, cell lysates were cleared by centrifugation at 12000 g for 25 min. All steps were carried out at 4°C. Lysates were incubated for 3h with 5 μL of biotinylated mouse monoclonal anti-Myc antibody or for 16 h with 1 μL of mouse monoclonal anti-GFP antibody (antibodies were obtained from Santa Cruz Biotechnology), and then for 45 min with streptavidin beads or protein G beads (Invitrogen) at 4°C, and washed twice with PBS/Tween-20 buffer, and twice with PBS. Beads were resuspended in 25 μL Laemmli buffer.

SDS-PAGE and immunoblot analysis

Immunoprecipitation samples, or total cell lysates (25 μg), were separated on 12 % or 4–20 % gradient (for $Ca_v3.2$) SDS-PAGE and transferred onto PVDF membrane (Millipore). For detection of the mCherry-tagged proteins, the membrane was incubated with a primary rabbit polyclonal anti-mCherry antibody (Abcam) diluted at 1:10.000; GFP-tagged proteins were detected with a primary rabbit polyclonal anti-GFP antibody (Abcam) diluted at 1:10.000; Myc-tagged Stac1 was detected with a biotinylated primary mouse monoclonal anti-Myc antibody (Santa Cruz Biotechnology) diluted at 1:2000. Membranes were then washed in PBS/Tween-20 buffer, and incubated with a secondary anti-rabbit HRP-conjugated antibody (Jackson ImmunoResearch) diluted at 1:10.000 or with the NeutrAvidin Protein HRP-conjugated (ThermoFisher Scientific) diluted at 1:10.000. For immunoprecipitation controls, membranes were stripped to remove antibodies in a stripping buffer (0.2 M glycine, 1 % SDS; pH 2.0) and then reblotted as described above. Immunoreactive bands were detected by enhanced chemiluminescence.

Surface immunostaining

Twenty-four hours before the experiment, cells expressing HA-$hCa_v3.2$ channels were seeded on poly-L-lysine-coated glass coverslips. Cells were incubated for 30 min at 37°C with a primary monoclonal mouse anti-HA antibody (Abcam) diluted in DMEM at 1:1000, washed with PBS, fixed for 7 min in 4 % paraformaldehyde, and blocked for 45 min in blocking buffer (5 % FBS in PBS). Cells were then incubated for 1 h at room temperature with a secondary goat polyclonal anti-mouse Alexa488-conjugated antibody (Jackson ImmunoResearch) diluted in blocking buffer at 1:1000, washed, and mounted on microscope glass slides with ProLong Gold mounting medium (Life Technologies). Confocal images were acquired at low magnification with a Zeiss LSM780 microscope and the field fluorescence intensity was analyzed using ImageJ software. In order to visualize intracellular channels, cells were permeabilized with 0.2 % Triton X-100 for 10 min before incubation with the secondary antibody.

Patch-clamp electrophysiology

Patch-clamp recordings were performed 72 h after transfection in the whole-cell configuration of the patch-clamp technique at room temperature (22–24°C) in a bath solution containing (in millimolar): 5 BaCl2, 5 KCl, 1 MgCl2, 128 NaCl, 10 TEA-Cl, 10 D-glucose, 10 4-(2-hydroxyethyl)-1-piperazineethanesulfonic acid (HEPES) (pH7.2 with NaOH). Patch pipettes had a resistance of 2–4 MΩ when filled with a solution containing (in millimolar): 110 CsCl, 3 Mg-ATP, 0.5 Na-GTP, 2.5 MgCl2, 5 D-glucose, 10 EGTA, and 10 HEPES (pH7.4 with CsOH). Whole-cell patch-clamp recordings were performed using an Axopatch 200B amplifier (Axon Instruments). Acquisition and

analysis were performed using pClamp 10 and Clampfit 10 software, respectively (Axon Instruments).

Ba^{2+} currents were recorded in response to 150 ms-long depolarizing to various potentials applied every 5 s from a holding potential of −100 mV. The linear leak component of the current was corrected online and current traces were digitized at 10 kHz, and filtered at 2 kHz. The voltage dependence of the peak Ba^{2+} current density was fitted with the following modified Boltzmann equation:

$$I(V) = Gmax\frac{(V - Vrev)}{1 + \exp\frac{(V0.5 - V)}{k}}$$

with $I(V)$ being the peak current amplitude at the command potential V, Gmax the maximum conductance, Vrev the reversal potential, $V_{0.5}$ the half-activation potential, and k the slope factor.

Statistical analysis

Data values are presented as mean ± SEM for n experiments. Statistical significance was determined using Student's unpaired t test: $^{*}p < 0.05$, $^{**}p < 0.01$, $^{***}p < 0.001$, and NS: statistically not different.

Disclosure of potential conflicts of interest

No potential conflicts of interest were disclosed.

Funding

Work in the Weiss laboratory is supported by the Czech Science Foundation (grant 15-13556S), the Czech Ministry of Education Youth and Sports (grant 7AMB15FR015), and the Institute of Organic Chemistry and Biochemistry (IOCB). YR, JL, and JP are supported by an IOCB postdoctoral fellowship. Work in the Flucher laboratory is supported by the Austrian Science Fund (FWF) (grant P27031 to BEF).

References

[1] Perez-Reyes, E. Molecular physiology of low-voltage-activated t-type calcium channels. Physiol Rev 2003; 83:117-61; PMID:12506128; http://dx.doi.org/10.1152/physrev.00018.2002

[2] Crunelli, V, Tóth, TI, Cope, DW, Blethyn, K, Hughes, SW. The 'window' T-type calcium current in brain dynamics of different behavioural states. J Physiol 2005; 562:121-9; PMID:15498803; http://dx.doi.org/10.1113/jphysiol.2004.076273

[3] Dreyfus, FM, Tscherter, A, Errington, AC, Renger, JJ, Shin, HS, Uebele, VN, Crunelli, V, Lambert, RC, Leresche, N. Selective T-type calcium channel block in thalamic neurons reveals channel redundancy and physiological impact of I(T)window. J Neurosci 2010; 30:99-109; PMID:20053892; http://dx.doi.org/10.1523/JNEUROSCI.4305-09.2010

[4] Crunelli, V, Cope, DW, Hughes, SW. Thalamic T-type Ca2+ channels and NREM sleep. Cell Calcium 2006; 40:175-90; PMID:16777223; http://dx.doi.org/10.1016/j.ceca.2006.04.022

[5] Bal, T, McCormick, DA. Synchronized oscillations in the inferior olive are controlled by the hyperpolarization-activated cation current I(h). J Neurophysiol 1997; 77:3145-56; PMID:9212264

[6] Beurrier, C, Congar, P, Bioulac, B, Hammond, C. Subthalamic nucleus neurons switch from single-spike activity to burst-firing mode. J Neurosci 1999; 19:599-609; PMID:9880580

[7] Sotty, F, Danik, M, Manseau, F, Laplante, F, Quirion, R, Williams, S. Distinct electrophysiological properties of glutamatergic, cholinergic and GABAergic rat septohippocampal neurons: novel implications for hippocampal rhythmicity. J Physiol 2003; 551:927-43; PMID:12865506; http://dx.doi.org/10.1113/jphysiol.2003.046847

[8] Cain, SM, Snutch, TP. T-type calcium channels in burst-firing, network synchrony, and epilepsy. Biochim Biophys Acta 2013; 1828:1572-8; PMID:22885138; http://dx.doi.org/10.1016/j.bbamem.2012.07.028

[9] Turner, RW, Zamponi, GW. T-type channels buddy up. Pflugers Arch 2014; 466:661-75; PMID:24413887; http://dx.doi.org/10.1007/s00424-013-1434-6

[10] Anderson, D, Mehaffey, WH, Iftinca, M, Rehak, R, Engbers, JD, Hameed, S, Zamponi, GW, Turner, RW. Regulation of neuronal activity by Cav3-Kv4 channel signaling complexes. Nat Neurosci 2010; 13:333-7; PMID:20154682; http://dx.doi.org/10.1038/nn.2493

[11] Rehak, R, Bartoletti, TM, Engbers, JD, Berecki, G, Turner, RW, Zamponi, GW. Low voltage activation of KCa1.1 current by Cav3-KCa1.1 complexes. PLoS One 2013; 8:e61844; PMID:23626738; http://dx.doi.org/10.1371/journal.pone.0061844

[12] Anderson, D, Engbers, JD, Heath, NC, Bartoletti, TM, Mehaffey, WH, Zamponi, GW, Turner, RW. The Cav3-Kv4 complex acts as a calcium sensor to maintain inhibitory charge transfer during extracellular calcium fluctuations. J Neurosci 2013; 33:7811-24; PMID:23637173; http://dx.doi.org/10.1523/JNEUROSCI.5384-12.2013

[13] Weiss, N, Hameed, S, Fernández-Fernández, JM, Fablet, K, Karmazinova, M, Poillot, C, Proft, J, Chen, L, Bidaud, I, Monteil, A, Huc-Brandt, S, Lacinova, L, Lory, P, Zamponi, GW, De Waard, M. A Ca(v)3.2/syntaxin-1A signaling complex controls T-type channel activity and low-threshold exocytosis. J Biol Chem 2012; 287:2810-8; PMID:22130660; http://dx.doi.org/10.1074/jbc.M111.290882

[14] Weiss, N, Zamponi, GW, De Waard, M. How do T-type calcium channels control low-threshold exocytosis. Commun Integr Biol 2012; 5:377-80; PMID:23060963; http://dx.doi.org/10.4161/cib.19997

[15] Jagodic, MM, Pathirathna, S, Nelson, MT, Mancuso, S, Joksovic, PM, Rosenberg, ER, Bayliss, DA, Jevtovic-Todorovic, V, Todorovic, SM. Cell-specific alterations of T-type calcium current in painful diabetic neuropathy enhance excitability of sensory neurons. J Neurosci 2007; 27:3305-16; PMID:17376991; http://dx.doi.org/10.1523/JNEUROSCI.4866-06.2007

[16] Jagodic, MM, Pathirathna, S, Joksovic, PM, Lee, W, Nelson, MT, Naik, AK, Su, P, Jevtovic-Todorovic, V, Todorovic, SM. Upregulation of the T-type calcium current in small rat sensory neurons after chronic constrictive injury of the sciatic nerve. J Neurophysiol 2008; 99:3151-6; PMID:18417624; http://dx.doi.org/10.1152/jn.01031.2007

[17] Latham, JR, Pathirathna, S, Jagodic, MM, Choe, WJ, Levin, ME, Nelson, MT, Lee, WY, Krishnan, K, Covey, DF, Todorovic, SM, Jevtovic-Todorovic, V. Selective T-type calcium channel blockade alleviates hyperalgesia in ob/ob mice. Diabetes 2009; 58:2656-65; PMID:19651818; http://dx.doi.org/10.2337/db08-1763

[18] Duzhyy, DE, Viatchenko-Karpinski, VY, Khomula, EV, Voitenko, NV, Belan, PV. Upregulation of T-type Ca2+ channels in long-term diabetes determines increased excitability of a specific type of capsaicin-insensitive DRG neurons. Mol Pain 2015; 11:29; PMID:25986602; http://dx.doi.org/10.1186/s12990-015-0028-z

[19] Watanabe, M, Ueda, T, Shibata, Y, Kumamoto, N, Shimada, S, Ugawa, S. Expression and Regulation of Cav3.2 T-Type Calcium Channels during Inflammatory Hyperalgesia in Mouse Dorsal Root Ganglion Neurons. PLoS One 2015; 10:e0127572; PMID:25974104; http://dx.doi.org/10.1371/journal.pone.0127572

[20] Yue, J, Liu, L, Liu, Z, Shu, B, Zhang, Y. Upregulation of T-type Ca2+ channels in primary sensory neurons in spinal nerve injury. Spine (Phila Pa 1976) 2013; 38:463-70; PMID:22972512; http://dx.doi.org/10.1097/BRS.0b013e318272fbf8

[21] Tsakiridou, E, Bertollini, L, de Curtis, M, Avanzini, G, Pape, HC. Selective increase in T-type calcium conductance of reticular thalamic neurons in a rat model of absence epilepsy. J Neurosci 1995; 15:3110-7; PMID:7722649

[22] Zhang, Y, Vilaythong, AP, Yoshor, D, Noebels, JL. Elevated thalamic low-voltage-activated currents precede the onset of absence epilepsy in the SNAP25-deficient mouse mutant coloboma. J Neurosci 2004; 24:5239-48; PMID:15175394; http://dx.doi.org/10.1523/JNEUROSCI.0992-04.2004

[23] Su, H, Sochivko, D, Becker, A, Chen, J, Jiang, Y, Yaari, Y, Beck, H. Upregulation of a T-type Ca2+ channel causes a long-lasting modification of neuronal firing mode after status epilepticus. J Neurosci 2002; 22:3645-55; PMID:11978840

[24] Powell, KL, Cain, SM, Ng, C, Sirdesai, S, David, LS, Kyi, M, Garcia, E, Tyson, JR, Reid, CA, Bahlo, M, Foote, SJ, Snutch, TP, O'Brien, TJ. A Cav3.2 T-type calcium channel point mutation has splice-variant-specific effects on function and segregates with seizure expression in a polygenic rat model of absence epilepsy. J Neurosci 2009; 29:371-80; PMID:19144837; http://dx.doi.org/10.1523/JNEUROSCI.5295-08.2009

[25] Tringham, E, Powell, KL, Cain, SM, Kuplast, K, Mezeyova, J, Weerapura, M, Eduljee, C, Jiang, X, Smith, P, Morrison, JL, Jones, NC, Braine, E, Rind, G, Fee-Maki, M, Parker, D, Pajouhesh, H, Parmar, M, O'Brien, TJ, Snutch, TP. T-type calcium channel blockers that attenuate thalamic burst firing and suppress absence seizures. Sci Transl Med 2012; 4:121ra19; PMID:22344687; http://dx.doi.org/10.1126/scitranslmed.3003120

[26] Casillas-Espinosa, PM, Hicks, A, Jeffreys, A, Snutch, TP, O'Brien, TJ, Powell, KL. Z944, a Novel Selective T-Type Calcium Channel Antagonist Delays the Progression of Seizures in the Amygdala Kindling Model. PLoS One 2015; 10:e0130012; PMID:26274319; http://dx.doi.org/10.1371/journal.pone.0130012

[27] Zhang, Y, Jiang, X, Snutch, TP, Tao, J. Modulation of low-voltage-activated T-type Ca^{2+} channels. Biochim Biophys Acta 2013; 1828:1550-9; PMID:22975282; http://dx.doi.org/10.1016/j.bbamem.2012.08.032

[28] Suzuki, H, Kawai, J, Taga, C, Yaoi, T, Hara, A, Hirose, K, Hayashizaki, Y, Watanabe, S. Stac, a novel neuron-specific protein with cysteine-rich and SH3 domains. Biochem Biophys Res Commun 1996; 229:902-9; PMID:8954993; http://dx.doi.org/10.1006/bbrc.1996.1900

[29] Polster, A, Perni, S, Bichraoui, H, Beam, KG. Stac adaptor proteins regulate trafficking and function of muscle and neuronal L-type Ca2+ channels. Proc Natl Acad Sci U S A 2015; 112:602-6; PMID:25548159; http://dx.doi.org/10.1073/pnas.1423113112

[30] Weiss, N. Stac gets the skeletal L-type calcium channel unstuck. Gen Physiol Biophys 2015; 34:101-3; PMID:25975219; http://dx.doi.org/10.4149/gpb_2015011

[31] Horstick, EJ, Linsley, JW, Dowling, JJ, Hauser, MA, McDonald, KK, Ashley-Koch, A, Saint-Amant, L, Satish, A, Cui, WW, Zhou, W, Sprague, SM, Stamm, DS, Powell, CM, Speer, MC, Franzini-Armstrong, C, Hirata, H, Kuwada, JY. Stac3 is a component of the excitation-contraction coupling machinery and mutated in Native American myopathy. Nat Commun 2013; 4:1952; PMID:23736855; http://dx.doi.org/10.1038/ncomms2952

[32] Nelson, BR, Wu, F, Liu, Y, Anderson, DM, McAnally, J, Lin, W, Cannon, SC, Bassel-Duby, R, Olson, EN. Skeletal muscle-specific T-tubule protein STAC3 mediates voltage-induced Ca2+ release and contractility. Proc Natl Acad Sci U S A 2013; 110:11881-6; PMID:23818578; http://dx.doi.org/10.1073/pnas.1310571110

[33] Bower, NI, de la Serrana, DG, Cole, NJ, Hollway, GE, Lee, HT, Assinder, S, Johnston, IA. Stac3 is required for myotube formation and myogenic differentiation in vertebrate skeletal muscle. J Biol Chem 2012; 287:43936-49; PMID:23076145; http://dx.doi.org/10.1074/jbc.M112.361311

[34] Legha, W, Gaillard, S, Gascon, E, Malapert, P, Hocine, M, Alonso, S, Moqrich, A. stac1 and stac2 genes define discrete and distinct subsets of dorsal root ganglia neurons.

Gene Expr Patterns 2010; 10:368-75; PMID:20736085; http://dx.doi.org/10.1016/j.gep.2010.08.003

[35] Simms, BA, Zamponi, GW. Trafficking and stability of voltage-gated calcium channels. Cell Mol Life Sci 2012; 69:843-56; PMID:21964928; http://dx.doi.org/10.1007/s00018-011-0843-y

[36] Dolphin, AC. Calcium channel auxiliary $\alpha 2\delta$ and β subunits: trafficking and one step beyond. Nat Rev Neurosci 2012; 13:542-55; PMID:22805911; http://dx.doi.org/10.1038/nrn3317

[37] Weiss, N, Black, SA, Bladen, C, Chen, L, Zamponi, GW. Surface expression and function of Cav3.2 T-type calcium channels are controlled by asparagine-linked glycosylation. Pflugers Arch 2013; 465:1159-70; PMID:23503728; http://dx.doi.org/10.1007/s00424-013-1259-3

[38] Lazniewska, J, Weiss, N. The "sweet" side of ion channels. Rev Physiol Biochem Pharmacol 2014; 167:67-114; PMID:25239698

[39] Ondacova, K, Karmazinova, M, Lazniewska, J, Weiss, N, Lacinova, L. Modulation of Cav3.2 T-type calcium channel permeability by asparagine-linked glycosylation. Channels (Austin) 2016; 10:175-84; PMID:26745591; http://dx.doi.org/10.1080/19336950.2016.1138189

[40] García-Caballero, A, Gadotti, VM, Stemkowski, P, Weiss, N, Souza, IA, Hodgkinson, V, Bladen, C, Chen, L, Hamid, J, Pizzoccaro, A, Deage, M, François, A, Bourinet, E, Zamponi, GW. The deubiquitinating enzyme USP5 modulates neuropathic and inflammatory pain by enhancing Cav3.2 channel activity. Neuron 2014; 83:1144-58; http://dx.doi.org/10.1016/j.neuron.2014.07.036

[41] Karmažínová, M, Jašková, K, Griac, P, Perez-Reyes, E, Lacinová, Ľ. Contrasting the roles of the I-II loop gating brake in CaV3.1 and Ca V3.3 calcium channels. Pflugers Arch 2015; 467(12):2519-27

[42] Weiss, N, Lacinova, L. T-type channels: release a brake, engage a gear. Channels 2015; 10(2):78–80.

[43] Vitko, I, Bidaud, I, Arias, JM, Mezghrani, A, Lory, P, Perez-Reyes, E. The I-II loop controls plasma membrane expression and gating of Ca(v)3.2 T-type Ca2+ channels: a paradigm for childhood absence epilepsy mutations. J Neurosci 2007; 27:322-30; PMID:17215393; http://dx.doi.org/10.1523/JNEUROSCI.1817-06.2007

[44] Baumgart, JP, Vitko, I, Bidaud, I, Kondratskyi, A, Lory, P, Perez-Reyes, E. I-II loop structural determinants in the gating and surface expression of low voltage-activated calcium channels. PLoS One 2008; 3:e2976; PMID:18714336; http://dx.doi.org/10.1371/journal.pone.0002976

[45] Altier, C, Garcia-Caballero, A, Simms, B, You, H, Chen, L, Walcher, J, Tedford, HW, Hermosilla, T, Zamponi, GW. The Cavβ subunit prevents RFP2-mediated ubiquitination and proteasomal degradation of L-type channels. Nat Neurosci 2011; 14:173-80; PMID:21186355; http://dx.doi.org/10.1038/nn.2712

[46] Waithe, D, Ferron, L, Page, KM, Chaggar, K, Dolphin, AC. Beta-subunits promote the expression of Ca(V)2.2 channels by reducing their proteasomal degradation. J Biol Chem 2011; 286:9598-611; PMID:21233207; http://dx.doi.org/10.1074/jbc.M110.195909

[47] Gadotti, VM, Caballero, AG, Berger, ND, Gladding, CM, Chen, L, Pfeifer, TA, Zamponi, GW. Small organic molecule disruptors of Cav3.2 - USP5 interactions reverse inflammatory and neuropathic pain. Mol Pain 2015; 11:12; PMID:25889575; http://dx.doi.org/10.1186/s12990-015-0011-8